The Open Civil Engineering Journal
DOI: 10.2174/0118741495498869260918114758, 2026, 20, e18741495498869
ISSN: 1874-1495

RESEARCH ARTICLE OPEN ACCESS

Flexural Strength of CFSS Beams with Single and Double Web Holes

Andy Prabowo[1,*], Ikhsan Prabowo[1] and Daniel T. W. Looi[2]

[1]Master of Civil Engineering Program, Universitas Tarumanagara Jakarta, Jakarta, Indonesia
[2]School of Engineering, Sunway University, Sunway, Malaysia

Abstract:

Introduction: Web openings in structural beams facilitate building services; however, their influence on cold-formed stainless steel (CFSS) members, particularly under multiple openings, remains underexplored. This study addresses the gap in understanding of how single and double web holes affect the flexural performance and failure behavior of CFSS beams.

Methods: A total of 90 finite element models of ferritic and lean duplex CFSS beams were analyzed using ABAQUS under four-point bending. Parameters included varied cross-sections, hole diameters (20–90% of web depth), and single or double openings. Results were compared with existing design rules using reliability analysis.

Results: Web openings up to 20% of web depth showed negligible impact on flexural strength. Increasing from one to two holes caused minimal additional strength reduction, though larger openings (≥50%) led to more pronounced capacity loss. All specimens failed by flexural buckling interacting with local buckling. Existing design methods yielded conservative predictions with safety indices exceeding the recommended minimum of 2.5.

Discussion: The minimal impact of multiple openings confirms the web's limited contribution to flexural resistance under pure bending, even considering stainless steel's nonlinear behavior. Current design rules remain reliable for beams with up to two openings.

Conclusion: CFSS beams can safely accommodate single or double web openings up to 20% of web depth without significant strength loss, enabling practical service integration while maintaining structural safety.

Keywords: Flexural strength, Cold-formed stainless steel, Rectangular hollow section, Lean duplex, Perforated beams, Direct strength method.

© 2026 The Author(s). Published by Bentham Open.
This is an open access article distributed under the terms of the Creative Commons Attribution 4.0 International Public License (CC-BY 4.0), a copy of which is available at: https://creativecommons.org/licenses/by/4.0/legalcode. This license permits unrestricted use, distribution, and reproduction in any medium, provided the original author and source are credited.

*Address correspondence to this author at the Master of Civil Engineering Program, Universitas Tarumanagara Jakarta, Jakarta, Indonesia; E-mail: andy.prabowo@ft.untar.ac.id

Cite as: Prabowo A, Prabowo I, Looi D. Flexural Strength of CFSS Beams with Single and Double Web Holes. Open Civ Eng J, 2026; 20: e18741495498869. http://dx.doi.org/10.2174/0118741495498869260918114758

Received: May 08, 2026
Revised: July 02, 2026
Accepted: July 15, 2026
Published: September 21, 2026

Send Orders for Reprints to
reprints@benthamscience.net

1. INTRODUCTION

Cold-formed stainless steel (CFSS) members are increasingly used in structural engineering due to their high strength-to-weight ratio, excellent corrosion resistance, and favorable durability characteristics [1-6]. These advantages contribute to reduced maintenance and extended service life, supporting sustainable infrastructure development in line with the United Nations Sustainable Development Goals, particularly Sustainable

Development Goal 9 and Sustainable Development Goal 11. However, unlike conventional carbon steel, CFSS exhibits pronounced material nonlinearity, which significantly influences buckling response, post-buckling behavior, and ultimate strength [7-9]. Among available grades, ferritic (EN 1.4003) and lean duplex (EN 1.4162) stainless steel have emerged as an efficient alternative due to their high strength, superior ductility, and cheaper market price due to a lower nickel content, particularly for EN 1.4162.

Previous studies have established a fundamental understanding of the structural behavior of cold-formed stainless steel members subjected to pure bending, particularly those fabricated from lean duplex stainless steel (LDSS) [10-12] and ferritic stainless steel (FSS) [13-15] grades. Subsequently, fewer investigations have been conducted on the structural performance of CFSS members at elevated temperature conditions [16-18]. Collectively, these investigations confirm that cold-formed stainless steel members exhibit complex interactions between local buckling, material nonlinearity, and geometric imperfections, which govern their ultimate strength.

In practical applications, web openings are frequently introduced in beam members to facilitate the integration of mechanical and electrical services. While such openings improve functional efficiency and can reduce overall structural depth, they also alter stress distribution and may trigger localized instability. Existing studies on CFSS members with web openings remain limited and are largely confined to configurations with a single opening [19-21]. Subsequently, investigations of CFSS beams with a single web opening at elevated temperatures have recently been conducted by Prabowo *et al.* [22] and Priestley and Prabowo [23]. The study by [22] evaluated the strength predictions of CFSS beams with a single web hole based on current design provisions, including ASCE [24], EC3 [25], and AS/NZS [26], using finite element analysis. Their results indicated that these design methods provide generally conservative and reliable predictions.

From a mechanics perspective, the assumption that the web contributes only minimally to flexural resistance suggests that multiple openings may have limited influence on bending strength. However, this assumption has not been rigorously validated for CFSS sections, where geometric slenderness and material nonlinearity may amplify local effects. Moreover, no comprehensive parametric study has been conducted that explicitly quantifies the influence of multiple web openings on the flexural behavior of CFSS beams under pure bending conditions. In addition, the reliability of existing design provisions for such configurations remains largely unexplored, particularly in terms of their ability to capture strength variations and failure mechanisms associated with multiple openings.

Addressing the current limitations on CFSS beams with multiple openings solely through experimental investigation alone is not only resource-intensive but also inherently limited in its ability to capture the wide range of geometric configurations and parameters involved. Consequently, relying solely on experimental data would result in a restricted and potentially non-generalizable understanding of the problem [27, 28]. In contrast, advanced numerical modeling offers a robust and efficient framework for systematically investigating these complex behaviors. When rigorously validated against experimental results, finite element analysis is capable of accurately capturing material nonlinearity, geometric imperfections, and local instability phenomena [29-33]. Moreover, it enables comprehensive parametric studies that are otherwise impractical to conduct experimentally [17, 33-36]. For these reasons, the use of validated numerical modelling is not only appropriate but necessary to provide a reliable and generalized assessment of the structural performance of perforated CFSS members [19, 36-38].

This study investigates the effects of single and double web holes on the pure bending strength of CFSS beams, fabricated from ferritic and lean duplex grades. The effects of the existence of multiple web holes on the strength reduction of CFSS beams under pure bending remain unexplored in existing studies [10-15, 19], while the requirement of multiple holes in the beams cannot be avoided in practice. Ultimate strengths obtained from finite element analyses conducted using ABAQUS [39] are presented to quantify the extent of strength degradation associated with multiple web openings. Furthermore, the numerical results are used to evaluate the applicability of existing design rules proposed by Chen *et al.* [19] and Prabowo *et al.* [23]. Reliability analyses are also performed to assess the safety and consistency of these design approaches when applied to beams with multiple web holes, thereby providing a more comprehensive basis for the design of perforated CFSS members.

2. RESEARCH METHOD

Numerical modelling of CFSS beams based on the study carried out by Prabowo *et al.* [22] was adopted for this study. Details of the numerical model, including the material modelling, finite element types, mesh sizes, and boundary conditions, can be found in the study [22]. The nonlinear material model used in this study was based on the laboratory test results conducted by Chen *et al.* [19] for the ferritic grade, and Huang and Young [40] for the lean duplex grade. Table **1** presents the extract of coupon test results, with E = Young's modulus (MPa), $f_{0.2}$ = yield strength (MPa), f_u = ultimate strength (MPa), and e_f = strain at failure. The strength enhancement that commonly takes place at the corner parts of the cross-section was incorporated into the model by considering the recommendation from [19]. The numerical model has been validated against the laboratory test results performed by Chen *et al.* [19]. Hence, results from the numerical analyses developed in ABAQUS are in close agreement with experimental results.

Table 1. Material properties of CFSS sections [11, 19].

Grades	Cross-section parts	E (MPa)	$f_{0.2}$ (MPa)	f_u (MPa)	e_f (%)
Ferritic (EN 1.4003)	Flat part	210000	410	466	13.1
	Corner part	205700	578	612	12.2
Lean duplex (EN 1.4162)	Flat part	197700	650	732.7	21.3
	Corner part	212300	893	1004.9	12.7

Upon validation of the numerical model, a parametric study was performed. The study was conducted based on numerical specimen variations, including the cross-section sizes, number of holes, and hole diameter. The typical cross-section of CFSS beams considered in the parametric study is depicted in Fig. (1), with the variations included in this study presented in Table 2, in which H = overall depth, B = overall width, t = thickness, r_o = outer radius, and r_i = inner radius of the corner. The hole diameter is expressed as a percentage of the flat depth (H-2t-2r_i) of the web. In this study, the web hole diameters relative to the flat depth consist of 20% (D20), 50% (D50), 70% (D70), and 90% (D90).

The positions of web holes are located in the moment region to ensure the failure occurs exclusively within this region. The moment is denoted as L2 in Figs. (2 and 3), while L1 in the figure is defined for the shear span. The distinction between moment span and shear span is necessary for the four-point loading simulation to obtain pure bending strength in the moment. The loading point is located at one- and two-thirds of the beam span, represented by the presence of stiffener plates. This is consistent with the experimental setup of Chen *et al.* [19]. The stiffener plates at the ends of the beam, including those at loading points, prevented local buckling during loading assignments. The holes were located in symmetrical positions. The magnitudes of L1 and L2 are provided in Table 3. Overall, L2 ranges from 3-5 times the larger cross-section dimensions, consistent with Chen *et al.* [19].

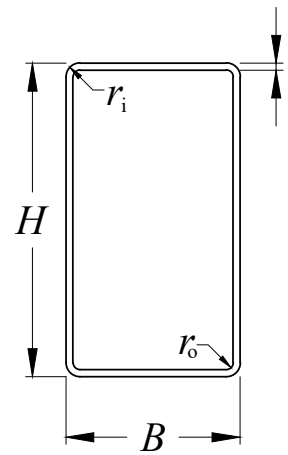

Fig. (1). Cross-section CFLDRHS.

Table 2. Cross-section variations for ferritic and lean duplex grades.

H (mm)	B (mm)	t (mm)	r_o (mm)	r_i (mm)	$(H-2(r_i+t))/t$	H/B
80	60	4.0	8.0	4.0	16	1.3
100	40	2.0	4.0	2.0	46	2.5
100	100	3	6	3	29.3	1.0
150	75	1.5	3	1.5	96	2.0
200	200	2.5	5	2.5	76	1.0

Table 3. Span of the specimens.

H (mm)	B (mm)	L1 (mm)	L2 (mm)	L3 (mm)
80	60	320	320	90
100	40	400	400	90
100	100	400	400	90
150	75	600	600	90
200	200	800	800	90

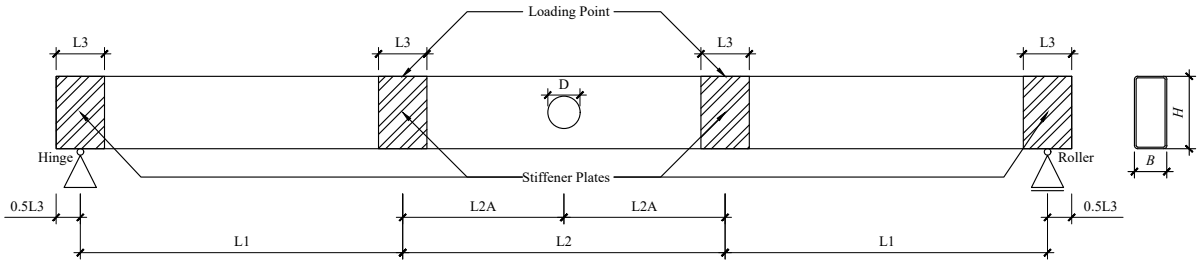

Fig. (2). Schematic of beam with single web hole.

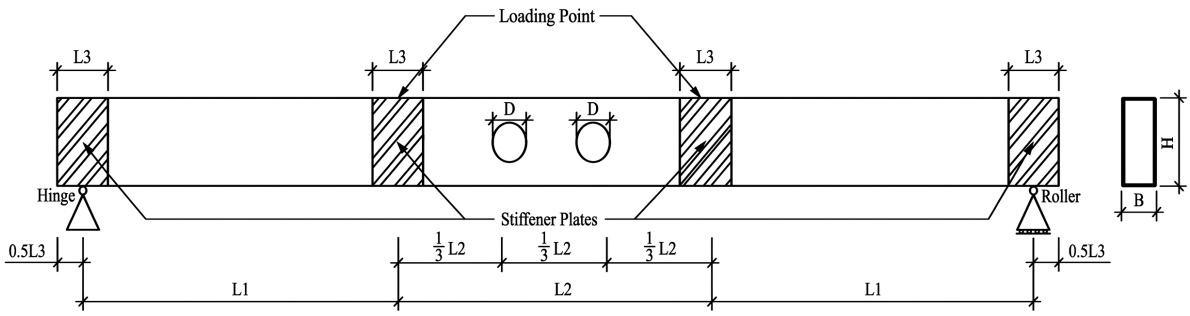

Fig. (3). Schematic of beam with double web holes.

3. RESULT AND DISCUSSION

3.1. Flexural Strength

Two primary results obtained from ABAQUS are summarised in this section, namely ultimate flexural strengths and failure modes. Table 4 presents the ultimate flexural strength from the finite element analyses (M_{FEA}), with $M_{FEA,\ F}$ denoting M_{FEA} for the ferritic sections and $M_{FEA,\ L}$ for lean duplex sections. It is obvious that the $M_{FEA,\ F}$ values are smaller than $M_{FEA,\ L}$ values due to material property differences. Table 4 shows that the presence of additional web holes does not cause a substantial strength reduction. As the hole diameter increases, an additional web hole only marginally reduces the strength due to stress redistribution in the hole perimeter, owing to the inherent ductility characteristics of stainless steel material [22].

Table 4. Ultimate flexural strength for sections with 1 and 2 holes.

$H \times B \times t$	% hole	$M_{FEA,\ F}$ (kNm)		$M_{FEA,\ L}$ (kNm)	
		1 hole	2 holes	1 hole	2 holes
80 × 60 × 4	D20	13.43	13.43	21.50	21.45
	D50	12.97	12.90	20.77	20.65
	D70	12.22	12.16	19.71	19.57
	D90	10.90	10.86	17.62	17.45
100 × 40 × 2	D20	7.54	7.54	11.46	11.46
	D50	6.98	6.96	10.61	10.61
	D70	6.22	6.17	9.83	9.74
	D90	4.94	5.58	7.68	8.60
100 × 100 × 3	D20	18.05	17.08	24.97	24.94
	D50	17.12	16.82	24.15	23.87
	D70	16.69	16.46	23.52	22.62
	D90	14.24	14.30	20.09	20.13
150 × 75 × 1.5	D20	8.29	8.44	12.18	12.28
	D50	7.93	8.02	12.52	12.63
	D70	7.44	7.36	12.22	12.36
	D90	5.98	5.90	8.98	9.15
200 × 200 × 2.5	D20	40.92	36.95	53.90	54.23
	D50	34.57	36.40	52.71	53.72
	D70	31.76	31.91	41.74	43.35
	D90	27.26	27.93	35.91	37.25

Comparisons between Tables **4** and **5** show that the strength reductions due to an additional hole are relatively minimal in specimens having a 20% hole diameter. The strength reductions become more pronounced as the hole sizes increase. In theory, the bending strength is mainly derived from the top and bottom flat parts of the cross-section in Fig. (**1**). The bending stress is maximum at these two parts, according to the principle of mechanics. The top part experiences compression stress ($f_{compression}$), while the bottom part experiences tension stress ($f_{tension}$). The force equilibrium is depicted on the right side of the figure, with C and T being the total compression and tension forces, respectively; these forces are located near the top and bottom fibers of the section. Therefore, it is understood that the presence of a web hole does not necessarily impact the strength reduction, especially when there are multiple holes in the beam web. This explanation can also be illustrated using (Fig. **4**). The larger the size of H or Z (moment lever arm), the less the influence of the beam web on the bending strength.

Table 5. Ultimate flexural strength for sections without a hole.

HxBxt	$M_{FEA,\ F}$ (kNm)	$M_{FEA,\ L}$ (kNm)
80 × 60 × 4	13.47	21.56
100 × 40 × 2	7.55	11.49
100 × 100 × 3	18.07	25.02
150 × 75 × 1.5	8.50	12.35
200 × 200 × 2.5	41.23	54.69

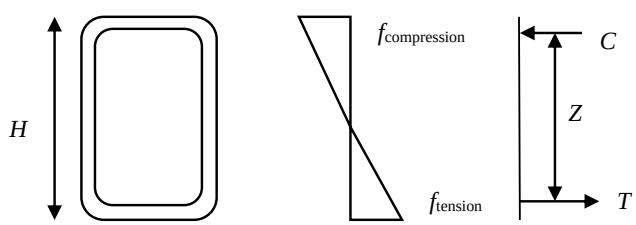

Fig. (4). Bending stress development in the beam.

3.2. Failure Modes

The failure modes obtained from ABAQUS are shown in Figs. (**5-7**). From these three figures, it is shown that no shear failure occurred in the shear span. In addition, all figures show bending failure occurring within the moment span, which was characterized by flexural buckling combined with local buckling.

3.3. Comparison with Strength Predictions

Three strength predictions were evaluated in this study, including those proposed by ASCE [24] (M_{ASCE}), Chen *et al.* [19] (M_C), and Priestley and Prabowo [23] (M_P). The values of M_{ASCE}, M_C, and M_P are obtained from M_n in Eq. (**1**), where M_{nl} is obtained from Eqs. (**2** and **3**), and M_{ynet} is obtained from Eq. (**4**). These three strength predictions are originally applicable to beams with a single web hole. Hence, this study investigates their applicability to beams with multiple web holes. Overall, these three strength predictions have similar equation formats as follows:

$$M_n = \min(M_{nl}, M_{ynet}) \quad \textbf{(1)}$$

$$\lambda_l \le \alpha \rightarrow \ M_{nl} = \kappa M_y$$
$$\lambda_l > \alpha \rightarrow \ M_{nl} = \left[\frac{\beta}{\lambda_l^{0.8}} - \frac{\gamma}{\lambda_l^{1.6}}\right] M_y \quad \textbf{(2)}$$

$$\lambda_l = \sqrt{\frac{M_{nl}}{M_{crl}}} \quad \textbf{(3)}$$

$$M_{ynet} = S_{net}\, f_{0.2} \quad \textbf{(4)}$$

where M_n = Nominal flexural strength of the beams without and with web holes; M_{ynet} = Flexural strength based on net section elastic modulus (S_{net}); M_{nl} = Flexural strength of section under combined local and flexural buckling mode; M_y = Yield moment of cross-sections ($S.f_{0.2}$); M_{crl} = Critical local buckling strength obtained from the CUFSM (Constrained and Unconstrained Finite Strip Method) tool; and are obtained from Table **6**.

Based on Table **6**, it is shown that the strength predictions prescribed by ASCE [24] are the most conservative since they do not account for the strength enhancement of a stocky section ($\lambda_l \le \alpha$). The other two strength predictions take into account the strength enhancement, as it permits $M_n > M_y$.

It has been mentioned above that the strength predictions require the M_{crl} value, which can be obtained using CUFSM software [41]. A preview of CUFSM results is shown in Fig. (**8**) for sections without a web hole (lean duplex 80 × 40 × 4), while sections with double web holes were treated as a single web hole (Fig. **9**) due to limitations of the CUFSM and for simplification. The rationale behind this simplification is that the bending stress along the moment span will be uniform under four-point loading.

Table 6. Values of *a* and *x* for the three strength predictions.

Strength Prediction/Refs.	α	β	γ	$\kappa \ge 1$
ASCE [24]	0.667	1	0.2	1
Chen *et al.* [19]	0.776	1	0.15	$1.5 - (0.5/0.776)\lambda_l$
Priestley and Prabowo [23]	0.667	0.8	0.2	$1.4 - \lambda_l$

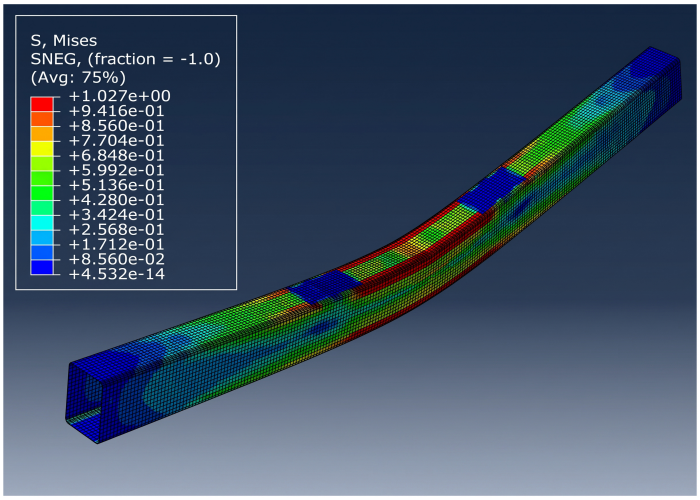

Fig. (5). Failure mode of section 80 × 40 × 4 without hole.

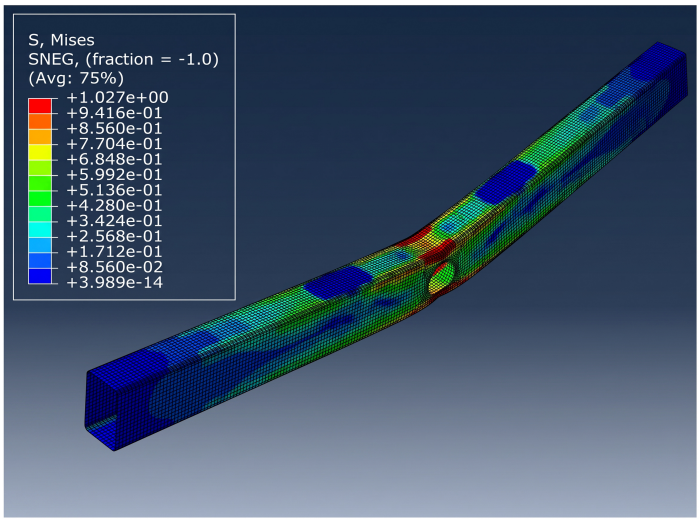

Fig. (6). Failure mode of section 80 × 40 × 4 with 1 web hole D70.

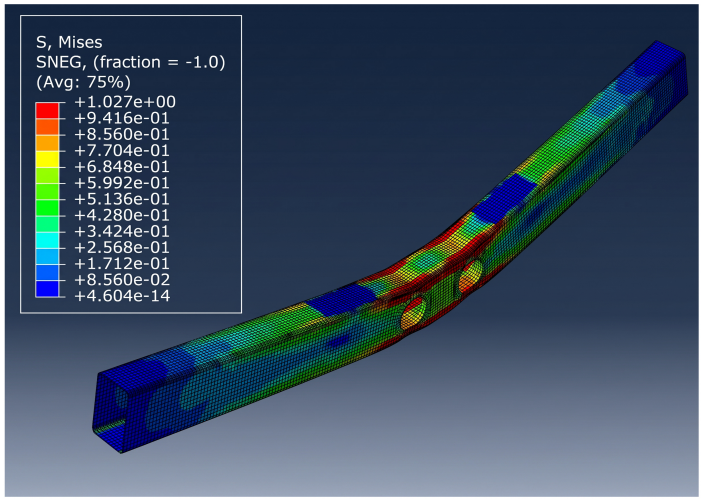

Fig. (7). Failure mode of section 80 × 40 × 4 with 2 web holes D70.

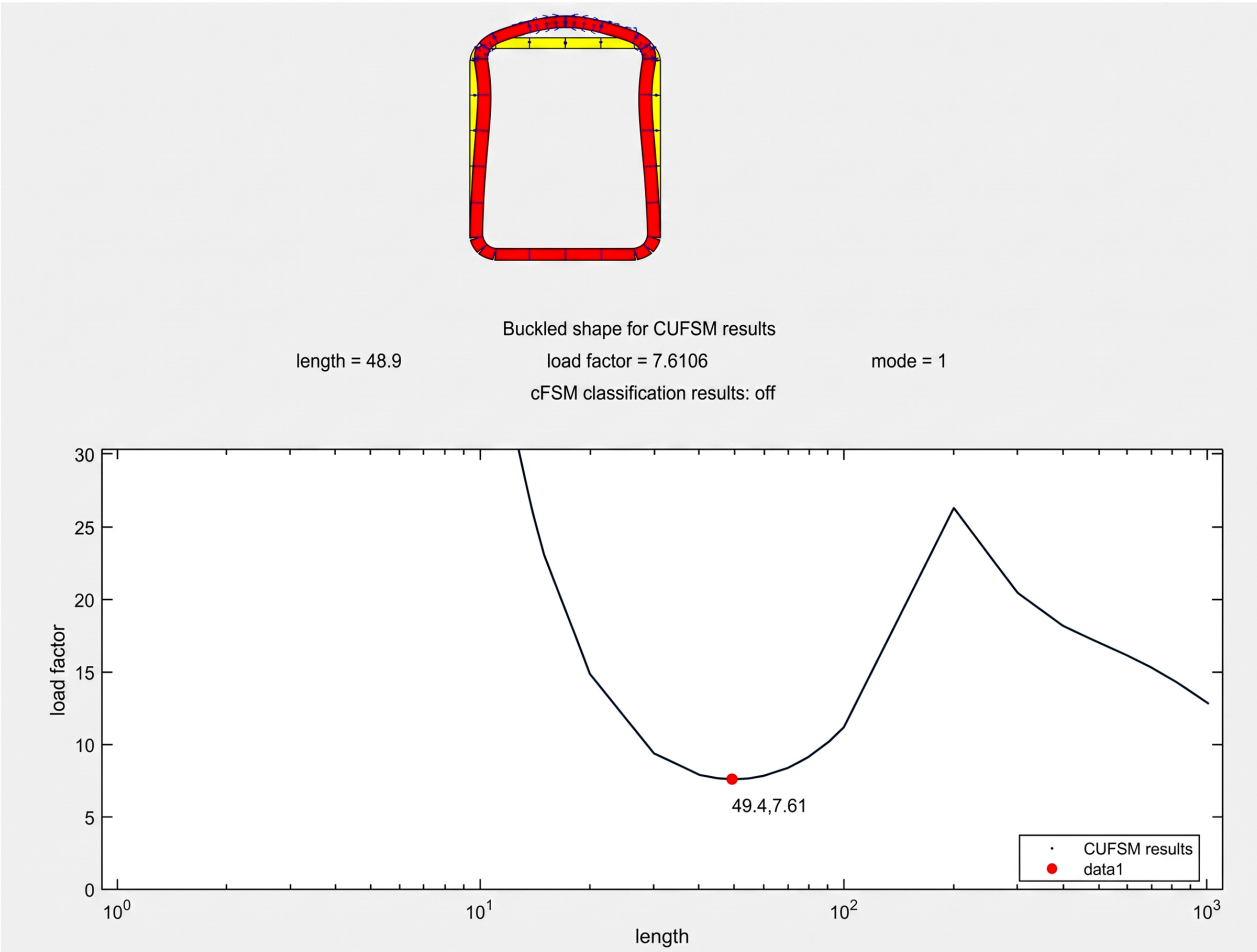

Fig. (8). CUFSM preview results for sections without a web hole.

From Figs. (**8** and **9**), the values of M_{crl} are shown at the lowest point of the curve, where indicated by a red dot. The first numbers (49.4 and 50.0) indicate the half-wave buckling length, while the second numbers (7.61 and 7.40) indicate the M_{crl} values. These values were then multiplied by M_y as an input to Eqs. (**2** and **3**). For sections with the web holes, the M_{crl} values obtained from CUFSM must be compared with M_{crl} values associated with the hole diameter read from the curve. More details regarding the determination of M_{crl} for sections with a web hole can be found in the study by Prabowo *et al*. [22]. In summary, the M_{crl} shall be obtained from the following considerations:

- If the hole diameter < half-wave buckling length obtained from the CUFSM calculation for sections with holes (like Fig. **9**), then M_{crl} equals the corresponding CUFSM calculation for sections without holes,
- Otherwise, the M_{crl} shall be taken from the CUFSM calculation for sections with holes.
- It should be noted that the M_{crl} value for sections with holes should not exceed the M_{crl} of sections without holes.

Evaluations of the three strength predictions were performed using the reliability analysis formula provided by ASCE [24], using the applicable load combination of 1.2 Dead Loads plus 1.6 Live Loads. Results from the comparison between M_{FEA} with M_{ASCE}, $M_{C,}$ and M_P are summarised in Table **7**. The purpose of this comparison is to demonstrate how conservative the three strength predictions are for the 90 variations that are used in this study. Moreover, the safety index (β_o) of the three strength predictions is obtained by using the reliability analysis. The magnitude of (β_o) is obtained from Chapter 11 of ASCE [24], which is primarily governed by the mean of the ratio between M_{FEA} and M_n (calculated from the three strength predictions) and the coefficient of variation (COV) of the ratio between M_{FEA} and M_n. A minimum (β_o) value of 2.5 must be achieved to determine that the strength prediction can be used safely.

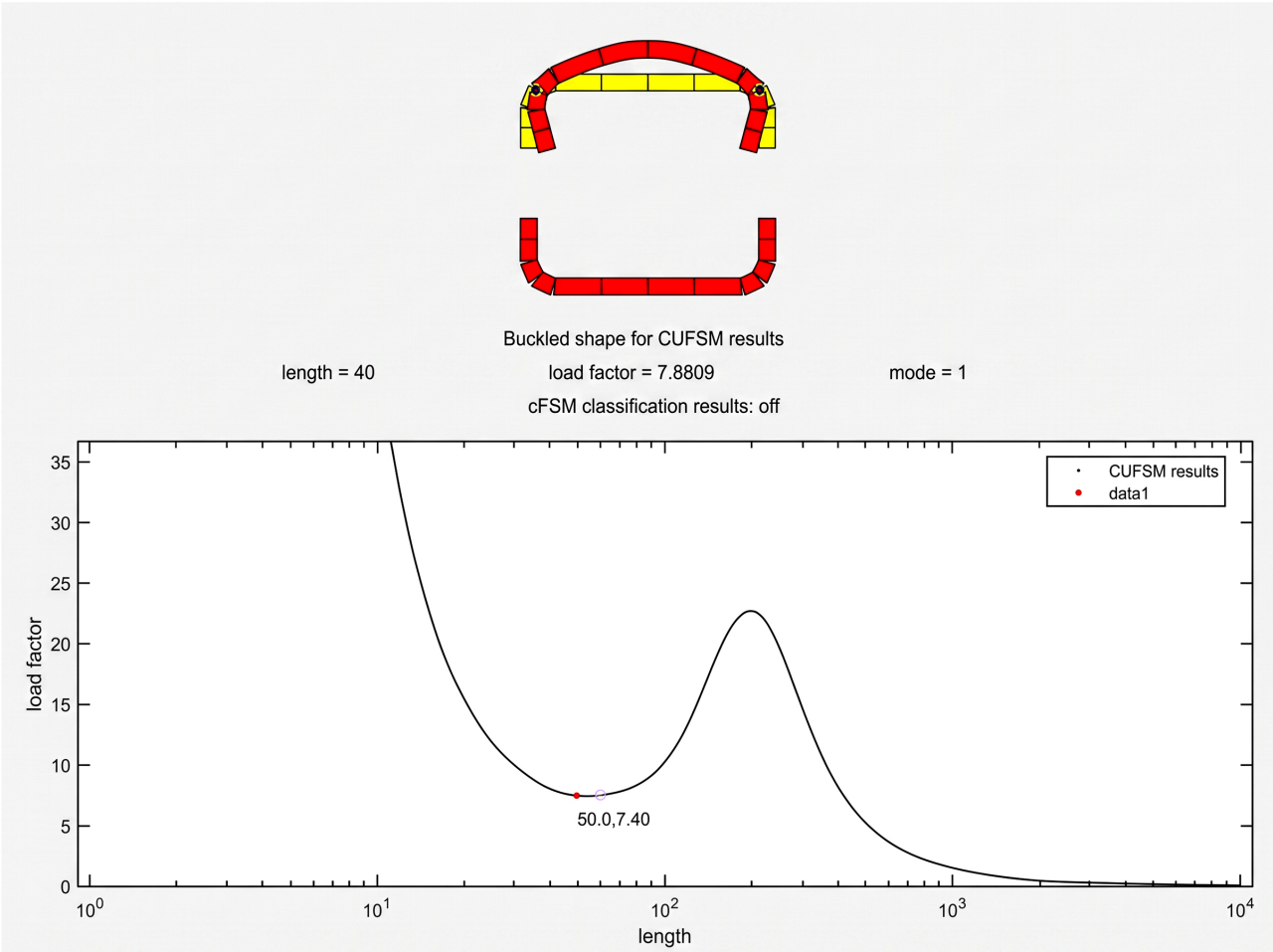

Fig. (9). CUFSM preview results for sections with a web hole.

Table 7. Evaluations of the three strength predictions for two grades of specimens.

Grades	Ferritic			Lean Duplex		
	$M_n = M_{ASCE}$	$M_n = M_C$	$M_n = M_P$	$M_n = M_{ASCE}$	$M_n = M_C$	$M_n = M_P$
Mean (M_{FEA}/M_n)	1.22	1.20	1.43	1.25	1.22	1.50
COV of M_{FEA}/M_n	0.164	0.181	0.110	0.128	0.145	0.098
ϕ	0.9	0.9	0.9	0.9	0.9	0.9
β_o	2.94	2.77	3.91	3.25	3.05	4.21

From Table 7, it is shown that the three strength predictions are conservative since the mean values are greater than 1, even though the stainless steel grades are different. The least conservative predictions were offered by Chen *et al.* [19], as indicated by the lowest mean value. However, the least scattered predictions were obtained from Prabowo *et al.* [22] strength prediction, as indicated by the smallest COV values. Moreover, when using the same strength reduction factor, the three strength predictions were found to be safely used, as the β_o values were greater than 2.5. The most optimum strength prediction came from the study by Chen *et al.* [19], since it had the lowest β_o values.

CONCLUSION

This paper presents an investigation into the flexural strength of cold-formed ferritic and lean duplex stainless steel beams under four-point loading with single and double web holes. A total of 90 numerical specimens were developed and analysed using finite element analysis. The pure bending strength was evaluated within the constant moment region, and all specimens exhibited failure governed by flexural buckling interacting with local buckling. The numerical results were used to assess the applicability of existing strength prediction methods for cold-formed stainless steel beams with web openings. The findings demonstrate that current design provisions provide conservative and safe predictions for beams with single and double web holes, as well as for beams without openings. The inclusion of single web hole cases enables a comprehensive evaluation of the design methods, and the calculated safety indices confirm the reliability of these approaches across different hole configurations.

STUDY LIMITATIONS

Despite these contributions, several limitations should be acknowledged. The study is based primarily on finite element modelling, and although validated against available experimental data, the validation was limited to specific cases. The investigation is also restricted to pure bending conditions, whereas practical structures may experience combined loading effects. In addition, the parametric scope was limited to selected cross-sections and opening configurations.

Future research should therefore focus on experimental validation of beams with multiple web openings, as well as investigations under combined loading conditions and more complex opening arrangements. The development of refined design methods that explicitly consider multiple openings is also recommended to further enhance the reliability and applicability of practical design approaches.

AUTHORS' CONTRIBUTIONS

The authors confirm their contributions to the paper as follows: A.P.: Study conception, design, analysis, interpretation of results, and manuscript editing; I.P.: Data collection, analysis, manuscript draft; D.T.W.L.: Supervision, manuscript editing. All authors reviewed the results and approved the final version of the manuscript under the heading of Author Contribution.

LIST OF ABBREVIATIONS

CFSS	=	Cold-Formed Stainless Steel
LDSS	=	Lean Duplex Stainless Steel
E	=	Young's modulus
$f_{0.2}$	=	yield strength
f_u	=	ultimate strength
e_f	=	strain at failure
H	=	overall depth
B	=	overall width
t	=	thickness
r_o	=	outer radius
r_i	=	inner radius of corner
H-2t-2r_i	=	flat depth
L1	=	shear span (left)
L2	=	moment span
L2A	=	one-third of moment span
L3	=	shear span (right)
FEA	=	Finite Element Analysis
$M_{FEA,\ F}$	=	Ultimate strength of ferritic beams obtained from FEA
$M_{FEA,\ L}$	=	Ultimate strength of lean duplex beams obtained from FEA
$f_{compression}$	=	compression stress
$f_{tension}$	=	tension stress
C	=	compression force
T	=	tension force
Z	=	lever arm
M_n	=	Nominal flexural strength of the beams without and with web holes
M_{ynet}	=	Flexural strength based on net section elastic modulus
S_{net}	=	Net section elastic modulus
M_{nl}	=	Flexural strength of section under combined local and flexural buckling mode
M_y	=	Yield moment of cross-sections
S	=	Elastic modulus
M_{crl}	=	Critical local buckling strength obtained from CUFSM
CUFSM	=	Constrained and Unconstrained Finite Strip Method
COV	=	Coefficient of Variation
ϕ	=	Strength reduction factor
β_o	=	Reliability index

CONSENT FOR PUBLICATION

Not applicable.

AVAILABILITY OF DATA AND MATERIALS

The data of current study are available from corresponding author, [A.P], on a reasonable request.

FUNDING

This research is supported by the research funding provided by the university through the Institute for Research and Community Service.

CONFLICT OF INTEREST

The authors declare no conflict of interest, financial or otherwise.

ACKNOWLEDGEMENTS

The first author acknowledges the contributions of the second author, as this paper presents part of his master's thesis. Computational analysis of using ABAQUS is facilitated by Tarumanagara Foundation.

REFERENCES

[1] G. Beulah Gnana Ananthi, K. Roy, A.M.M. Ahmed, and J.B.P. Lim, "Non-linear behaviour and design of web stiffened battened built-up stainless steel channel sections under axial compression", *Structures,* vol. 30, pp. 477-494, 2021. [http://dx.doi.org/10.1016/j.istruc.2021.01.014]

[2] K. Roy, H. Lau, Z. Fang, A. Ahmed, and J.B.P. Lim, "Axial capacity of back-to-back built-up cold-formed stainless steel unlipped channels-Numerical investigation and parametric study", *Steel Compos. Struct.,* vol. 40, p. 761, 2021. [http://dx.doi.org/10.12989/scs.2021.40.5.761]

[3] B. Karabulut, G. Ferraz, and B. Rossi, "Lifecycle cost assessment of high strength carbon and stainless steel girder bridges", *J. Environ. Manage.,* vol. 277, p. 111460, 2021. [http://dx.doi.org/10.1016/j.jenvman.2020.111460] [PMID: 33254842]

[4] B.W. Schafer, R.S. Glauz, and H. Chen, "Revision of ASCE 8 - Design of cold-formed stainless steel structural members", *J. Construct. Steel Res.,* vol. 208, p. 107986, 2023. [http://dx.doi.org/10.1016/j.jcsr.2023.107986]

[5] H.T. Li, C.C. Jin, Q.Y. Li, and B. Young, "Experimental investigation of cold-formed stainless steel built-up closed section stub columns", *Eng. Struct.,* vol. 306, p. 117657, 2024. [http://dx.doi.org/10.1016/j.engstruct.2024.117657]

[6] Y. Huang, J. Yang, R. Feng, and H. Chen, "Resistance of cold-formed sorbite stainless steel circular tubes under uniaxial compression", *Thin-walled Struct.,* vol. 179, p. 109739, 2022. [http://dx.doi.org/10.1016/j.tws.2022.109739]

[7] Y. Yang, S. Niu, and X. Zhi, "DSM formula for local-global interaction buckling of cold-formed stainless steel I-beams", *Sustainability,* vol. 15, no. 2, p. 1333, 2023. [http://dx.doi.org/10.3390/su15021333]

[8] F. Zhou, L. Huang, and H.T. Li, "Cold-formed stainless steel SHS and RHS columns subjected to local-flexural interactive buckling", *J. Construct. Steel Res.,* vol. 188, p. 106999, 2022. [http://dx.doi.org/10.1016/j.jcsr.2021.106999]

[9] Z. He, Y. Zhang, X. Zhou, B. Zou, and Z. Zhang, "Post-buckling behavior and DSM design of cold-formed steel lipped channel columns experiencing local-distortional-global interaction", *Structures,* vol. 67, p. 106945, 2024. [http://dx.doi.org/10.1016/j.istruc.2024.106945]

[10] M. Theofanous, and L. Gardner, "Experimental and numerical studies of lean duplex stainless steel beams", *J. Construct. Steel Res.,* vol. 66, no. 6, pp. 816-825, 2010. [http://dx.doi.org/10.1016/j.jcsr.2010.01.012]

[11] Y. Huang, and B. Young, "Experimental and numerical investigation of cold-formed lean duplex stainless steel flexural members", *Thin-walled Struct.,* vol. 73, pp. 216-228, 2013. [http://dx.doi.org/10.1016/j.tws.2013.07.019]

[12] I. Arrayago, and K.J.R. Rasmussen, "Buckling curves for cold-formed stainless-steel columns and beams", *J. Struct. Eng.,* vol. 147, no. 10, p. 04021149, 2021. [http://dx.doi.org/10.1061/(ASCE)ST.1943-541X.0003084]

[13] L. Li, H.T. Li, and B. Young, "Cold-formed ferritic stainless steel SHS and RHS beams: Testing, modeling and design", *J. Construct. Steel Res.,* vol. 197, p. 107429, 2022. [http://dx.doi.org/10.1016/j.jcsr.2022.107429]

[14] C. Karthik, and M. Anbarasu, "Cold-formed ferritic stainless steel closed built-up beams: Flexural behaviour and numerical parametric study", *Thin-walled Struct.,* vol. 164, p. 107816, 2021. [http://dx.doi.org/10.1016/j.tws.2021.107816]

[15] C. Karthik, M. Anbarasu, and M.A. Dar, "Reliable design rules for cold-formed ferritic stainless steel closed built-up beams", *Adv. Struct. Eng.,* vol. 27, no. 5, pp. 722-742, 2024. [http://dx.doi.org/10.1177/13694332241232046]

[16] Y. Huang, and B. Young, "Structural performance of cold-formed lean duplex stainless steel beams at elevated temperatures", *Thin-walled Struct.,* vol. 129, pp. 20-27, 2018. [http://dx.doi.org/10.1016/j.tws.2018.03.031]

[17] Y. Huang, J. Chen, Y. He, and B. Young, "Design of cold-formed stainless steel RHS and SHS beam–columns at elevated temperatures", *Thin-walled Struct.,* vol. 165, p. 107960, 2021. [http://dx.doi.org/10.1016/j.tws.2021.107960]

[18] H.T. Li, and B. Young, "Cold-formed high strength steel SHS and RHS beams at elevated temperatures", *J. Construct. Steel Res.,* vol. 158, pp. 475-485, 2019. [http://dx.doi.org/10.1016/j.jcsr.2019.03.034]

[19] Z. Chen, Y. Huang, and B. Young, "Design of cold-formed ferritic stainless steel RHS perforated beams", *Eng. Struct.,* vol. 250, p. 113372, 2022. [http://dx.doi.org/10.1016/j.engstruct.2021.113372]

[20] K.H. Lepcha, A.L. Marbaniang, M.L. Patton, and A. Khyriemmujat, "Behaviour and design of lean duplex stainless steel (LDSS) beams with web openings under pure bending", *Int. J. Steel Struct.,* vol. 20, no. 3, pp. 1052-1068, 2020. [http://dx.doi.org/10.1007/s13296-020-00342-4]

[21] K.H. Lepcha, and M.L. Patton, "A numerical study on structural behaviour of lean duplex stainless steel tubular beams with rectangular web openings", *Structures,* vol. 32, pp. 1233-1249, 2021. [http://dx.doi.org/10.1016/j.istruc.2021.01.081]

[22] A. Prabowo, Y. Huang, and B. Young, "Cold-formed stainless steel beams with single web hole at elevated temperatures", *Thin-walled Struct.,* vol. 195, p. 111321, 2024. [http://dx.doi.org/10.1016/j.tws.2023.111321]

[23] K.A. Priestley, and A. Prabowo, "Flexural strength of rhs perforated lean duplex stainless steel beam at temperature 24-900ºC", *Civ. Eng. Dimens.,* vol. 26, no. 1, pp. 71-80, 2024. [http://dx.doi.org/10.9744/ced.26.1.71-80]

[24] ASCE, *SEI/ASCE8-22: Specification for the design of cold-formed stainless steel structural members,* American Society of Civil Engineers: Reston, Virginia, 2022.

[25] CEN, *EN1993-1-4: Design of steel structures-part 1-4: General rules-supplementary rules for stainless steels,* European Committee for Standardization: Brussels, Belgium, 2006.

[26] AS/NZS, *AS/NZS 4673:2001: Cold-formed stainless steel structures,* Standards Australia/Standards New Zealand: Sydney, NSW, 2001.

[27] G.B.G. Ananthi, K. Roy, and J.B.P. Lim, "Tests and finite element modelling of cold-formed steel zed and hat section columns under axial compression", *Int. J. Steel Struct.,* vol. 21, no. 4, pp. 1305-1331, 2021. [http://dx.doi.org/10.1007/s13296-021-00504-y]

[28] X. Meng, and L. Gardner, "Cross-sectional behaviour of cold-formed high strength steel circular hollow sections", *Thin-walled Struct.,* vol. 156, p. 106822, 2020. [http://dx.doi.org/10.1016/j.tws.2020.106822]

[29] J. Dobrić, J. Ivanović, and B. Rossi, "Behaviour of stainless steel plain channel section columns", *Thin-walled Struct.,* vol. 148, p. 106600, 2020. [http://dx.doi.org/10.1016/j.tws.2020.106600]

[30] D. Jindra, Z. Kala, and J. Kala, "Validation of stainless-steel CHS columns finite element models", *Materials,* vol. 14, no. 7, p. 1785, 2021. [http://dx.doi.org/10.3390/ma14071785] [PMID: 33916591]

[31] F. Walport, H.U. Chan, D.A. Nethercot, and L. Gardner, "Design of stainless steel structural systems by GMNIA with strain limits",

Eng. Struct., vol. 276, p. 115339, 2023. [http://dx.doi.org/10.1016/j.engstruct.2022.115339]

[32] K. Ning, L. Yang, J. Wang, P. Dai, and Y. Sun, "Experimental and numerical study of hot-rolled duplex stainless steel CHS columns", *J. Construct. Steel Res.,* vol. 180, p. 106579, 2021. [http://dx.doi.org/10.1016/j.jcsr.2021.106579]

[33] C. Kyprianou, P. Kyvelou, L. Gardner, and D.A. Nethercot, "Finite element modelling of sheathed cold-formed steel beam–columns", *Thin-walled Struct.,* vol. 183, p. 110365, 2023. [http://dx.doi.org/10.1016/j.tws.2022.110365]

[34] M. Hasanali, S.M. Mojtabaei, I. Hajirasouliha, G.C. Clifton, and J.B.P. Lim, "More accurate design equations for cold-formed steel members subjected to combined axial compressive load and bending", *Thin-walled Struct.,* vol. 185, p. 110588, 2023. [http://dx.doi.org/10.1016/j.tws.2023.110588]

[35] S. Elglaad, M. Elghandour, T. Sharaf, and A. Elsabbagh, "Assessment of the finite element analysis of portal steel frames with cold formed rectangular hollow sections including imperfections and residual", *Port-Said Eng. Res. J.,* vol. 25, no. 2, p. 60-79, 2021. [http://dx.doi.org/10.21608/pserj.2021.75314.1111]

[36] N. Degtyareva, P. Gatheeshgar, K. Poologanathan, S. Gunalan, K.D. Tsavdaridis, and S. Napper, "New distortional buckling design rules for slotted perforated cold-formed steel beams", *J. Construct. Steel Res.,* vol. 168, p. 106006, 2020. [http://dx.doi.org/10.1016/j.jcsr.2020.106006]

[37] C. Yazıcı, and M. Gürbüz, "Experimental and numerical study of cold-formed steel beams with web perforations", *J. Struct. Eng. Appl. Mech.,* vol. 7, no. 3, pp. 172-185, 2024. [http://dx.doi.org/10.31462/jseam.2024.03172185]

[38] A.M. Yousefi, B. Samali, and Y. Yu, "Localised web bearing behaviour of cold-formed austenitic stainless-steel channels: Review of design rules and new insight under interior loading", *Appl. Sci.,* vol. 13, no. 19, p. 10696, 2023. [http://dx.doi.org/10.3390/app131910696]

[39] ABAQUS, *Standard user's manual,* Dassault Syst`emes Simulia Corp., 2023.

[40] Y. Huang, and B. Young, "The art of coupon tests", *J. Construct. Steel Res.,* vol. 96, pp. 159-175, 2014. [http://dx.doi.org/10.1016/j.jcsr.2014.01.010]

[41] B.W. Schafer, and S. Ádány, "Buckling analysis of cold-formed steel member using cufsm: Conventional and constrained finite strip methods", *Eighteenth International Specialty Conference on Cold-Formed Steel Structures,* 2006pp. 39-54 Orlando, Florida